JOC The Journal of Organic Chemistry

Article

pubs.acs.org/joc

Relative Stability and Diatropic Character of Carbaporphyrin, Dicarbaporphyrin, Tricarbaporphyrin, and Quatyrin Tautomers

Deyaa I. AbuSalim and Timothy D. Lash*

Department of Chemistry, Illinois State University, Normal, Illinois 61790-4160

Supporting Information

ABSTRACT: Monocarbaporphyrins, dicarbaporphyrins, tricarbaporphyrins, and quatyrins can all potentially exist in a number of tautomeric forms, but little is known about these species. In addition, no examples of tricarbaporphyrins or quatyrins are known at this time. In order to get information on the relative stabilities of carbaporphyrin tautomers, a series of aromatic and nonaromatic structures were assessed using computational methods. The conformations of 41 carbaporphyrin structures, together with four tautomers of porphyrin and the related antiaromatic species didehydroquatyrin, were minimized using DFT-B3LYP/6-311++G(d,p). The relative stabilities of the tautomers for each series were computed, and the bond lengths and bond angles were calculated. Many aromatic carbaporphyrin structures have very crowded cavities with up to six hydrogens being present. However, this was not sufficient to destabilize the aromatic structures relative to the nonaromatic forms. Furthermore, nucleus-independent chemical shifts (NICS) demonstrated that all of the porphyrinoids with 18-π-electron delocalization pathways are highly diatropic. *adj*-Dicarbaporphyrin and tricarbaporphyrin favor tautomers with an internal methylene group, while two interior methylenes are present in the favored tautomers for quatyrin. The results provide valuable information that will be helpful in designing synthetic routes to higher carbaporphyrinoid systems.

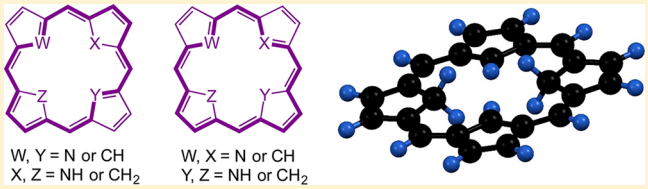

INTRODUCTION

Porphyrins serve numerous roles in nature, acting as superior ligands for transition-metal cations and providing a robust conjugated macrocycle that is virtually ubiquitous to living organisms.[1] In addition, porphyrins and related macrocycles have numerous applications in diverse areas that range from medicine to materials science.[2] The aromatic properties of porphyrins are well-known, but the origins of these characteristics are still debated.[3] Although many of the characteristics of porphyrinoids can be predicted by identifying a major conjugation pathway within the system,[3,4] theoretical studies have demonstrated that the observed properties of these systems are due to a superimposition of all of the possible conjugation pathways.[5−15] Furthermore, these studies indicate that the aromatic stabilization of porphyrinoids is primarily due to the aromatic character of the individual 6-π-electron subunits.[12,16] Hence, the [18]annulene model for porphyrinoid aromaticity does not appear to be a useful predictor for thermodynamic stability, although it does provide insights into the spectroscopic characteristics of these systems.[16]

For some years, we have been investigating the synthesis and characterization of carbaporphyrins and related conjugated macrocycles.[17,18] In principle, one, two, three, or four of the nitrogens in the porphyrin macrocycle could be replaced with carbon atoms to give monocarbaporphyrins (**CP**s), *opp*-dicarbaporphyrins (***opp*-DCP**s), *adj*-dicarbaporphyrins (***adj*-DCP**s), tricarbaporphyrins (**TCP**s), or tetracarbaporphyrins.[19] The aromatic tautomers of the last group have been named quatyrin (**Q**) and isoquatyrin,[19] and these represent theoretically important hydrocarbon analogues of the porphyrins.[20] Many examples of monocarbaporphyrins have been reported, including carbaporphyrin aldehydes **1**[21,22] and benzocarbaporphyrins **2**,[22−24] but far less work has been carried out on dicarbaporphyrins,[20] and tricarbaporphyrins and quatyrins are presently unknown. NMR spectroscopy has demonstrated that **1** and **2** favor a single tautomeric form,[22−24] and in the case of benzocarbaporphyrins **2** this has been unambiguously shown to correspond to the depicted structure.[24] Furthermore, ^4J coupling constants indicate that the C12−C13 bond possesses greater double-bond character in comparison to the C7−C8 and C17−C18 bonds, in line with expectations for structures possessing an 18-π-electron delocalization pathway.[24] The reactivity of carbaporphyrins has been studied in some detail, and these systems have been shown to undergo selective oxidations[25] and to act as organometallic ligands for Ag(III),[26] Au(III),[26,27] and Pd(II).[28,29] In addition, the protonation behavior of this system has been studied and both N-protonation and C-protonation has been observed.[22] However, experimental studies have so far not allowed the stability of tautomeric species to be investigated, and no information on the aromatic characteristics of ***adj*-DCP**, **TP**, and **Q** are available, as these systems have not yet been prepared. In order to assess these structures, we have turned to theoretical investigations so that the feasibility of synthesizing these porphyrinoids could be assessed. Very few computational

Received: September 24, 2013
Published: October 28, 2013

dx.doi.org/10.1021/jo4021198 | J. Org. Chem. 2013, 78, 11535−11548

studies have been carried out previously on carbaporphyrins, although tautomers of related N-confused porphyrins and higher order confused porphyrinoids have been thoroughly investigated by this approach.[30−32] Ghosh conducted density functional theory calculations on monocarbaporphyrin and predicted the geometry of the major tautomer and the relative energies of several protonated structures.[33−35] Feng and coworkers assessed the geometry and electronic structures of the major tautomers for **CP**, ***opp*-DCP**, and ***adj*-DCP**.[36,37] Although calculations were performed on "tricarbaporphyrin" and "tetracarbaporphyrin", these structures did not correspond to the correct oxidation level.[38] Calculations on didehydroquatyrin **3** have been performed previously,[38] and we have also investigated this potentially antiaromatic system. Finally, the structure of quatyrin has also been assessed by Salvi and coworkers.[39] In this work, 41 carbaporphyrin tautomers have been investigated using density functional theory and the diatropic character of these structures has been assessed by using nucleus-independent chemical shifts (NICSs). These investigations provide useful insights into the accessibility of various tautomeric forms, some of which may be involved in the metalation of these structures.

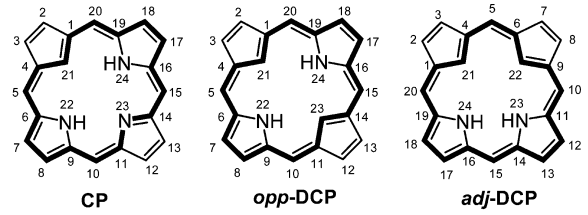

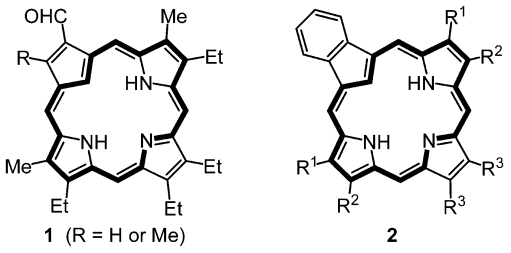

1 (R = H or Me) **2**

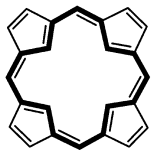

3 (Didehydroquatyrin)

RESULTS AND DISCUSSION

Monocarbaporphyrins. The relative stabilities of a series of monocarbaporphyrin tautomers were assessed using density functional theory (DFT) calculations. In essence, these structures differ by the positioning of two hydrogens that reside at positions 22 and 24 in the original structure. The tautomers are labeled to indicate the positions of these hydrogens, so that the first structure is considered to be **CP-22,24-H**. A total of 12 tautomers were considered for the monocarbaporphyrin series. In order to make comparisons, four tautomers of porphyrin (**P-21,23-H**, **P-21,22-H**, **P-5,21-H**, and **P-10,21-H**) were also assessed; **P-5,21-H** and **P-10,21-H** are nonaromatic isoporphyrin structures. As the thermodynamic stability of porphyrinoid structures may not necessarily be dependent on the presence of an 18-π-electron delocalization pathway, the comparative stabilities of formally nonaromatic tautomers will be a useful guide in future studies. Different levels of theory were initially tested, in order to find the optimal method out of those tested. These tests were performed by minimizing the structures of porphyrin **P-21,23-H** and carbaporphyrin **CP-22,24-H**, followed by comparing their corresponding geometries to each other as well as current literature data.[33,40] Test calculations were run using HF, DFT, and BP86 levels of theory with basis sets ranging from 6-31G(d,p) to cc-pVDZ. DFT-B3LYP/6-311++G(d,p) was found to be the optimum method, and hence it was utilized in the geometry optimization calculations. The calculations show that **P-21,23-H** is planar, while the other three porphyrin tautomers are only slightly twisted from planarity (for the dihedral angles, see Table 1). Carbaporphyrin **CP-22,24-H** is significantly distorted due to crowding within the macrocyclic cavity (Figure 1), and the cyclopentadiene subunit is rotated by 15° relative to the mean macrocyclic plane (Table 2). This is consistent with the X-ray crystal structure for the benzocarbaporphyrin **2**,[22] which shows that the indene unit is pivoted by 15.5° relative to the mean macrocyclic plane. On the other hand, tautomers **CP-21,23-H** (Figure 1) and **CP-21,22-H** are predicted to be planar. These structures possess an internal methylene group, and as these hydrogens will be placed above and below the plane of the macrocycle, this greatly decreases the steric interactions. Surprisingly, some of the nonaromatic structures (e.g., **CP-5,24-H**) are near planar as well. The calculated bond lengths and angles for the fully conjugated porphyrin and monocarbaporphyrin tautomers are shown in Figure 2. The values for porphyrin **P-21,23-H** are in accord with previous computational studies, and the results obtained for **CP-22,24-H** are in good agreement with DFT calculations reported by Ghosh et al.[30] All of the aromatic structures show bond lengths that are consistent with a fully delocalized aromatic system, although the reduced symmetry in these structures leads to some minor variations. Steric crowding within the macrocycles varies significantly. **P-21,23-H** has two internal hydrogens that are separated by 2.198 Å; in addition, the alternating arrangement of hydrogens optimizes hydrogen-bonding interactions and minimizes lone pair−lone pair repulsion. The less favored tautomer **P-21,22-H** has the two inner hydrogens closer together with a separation of 2.065 Å. The presence of three inner hydrogens in **CP-22,24-H** is more problematic, as the separation of the CH from the two NH units is only 1.863 Å. Nevertheless, the arrangement allows for the most favorable hydrogen-bonding interactions. In **CP-21,23-H**, where an internal methylene unit is present, the NH to CH distance is increased to 2.448 Å, thereby removing any significant crowding issues. However, this is less effective in tautomer **CP-21,22-H**, and in **CP-22,23-H** all three hydrogens are forced to be closer together.

The relative energies of the tautomers were calculated, and these are discussed below (Tables 3 and 4). For the porphyrin tautomers, **P-21,23-H** is the most stable, in accord with other

dx.doi.org/10.1021/jo4021198 | J. Org. Chem. 2013, 78, 11535−11548

Table 1. Dihedral Angles (deg) between the Four Five-Membered Rings in Each Macrocycle

structure	dihedral *ab*	dihedral *bc*	dihedral *cd*	dihedral *da*
P-21,23-H	0.00	0.00	0.00	0.00
P-21,22-H	−0.01	−0.04	0.01	0.05
P-5,21-H	0.02	−0.02	0.04	−0.02
P-10,21-H	−0.47	0.11	−0.16	0.45
CP-22,24-H	−11.56	1.52	−1.59	11.69
CP-21,23-H	0.00	0.00	0.00	0.00
CP-22,23-H	8.51	−0.53	5.07	−12.77
CP-21,22-H	0.00	0.00	0.00	0.00
CP-5,23-H	0.12	−0.02	0.02	−0.10
CP-5,22-H	11.37	−2.95	0.72	−6.40
CP-5,24-H	−0.03	0.07	0.00	−0.03
CP-10,23-H	0.39	−0.06	−0.07	−0.25
CP-10,24-H	0.03	−0.11	−0.03	0.06
CP-10,22-H	0.06	−0.11	0.20	−0.12
CP-10,21-H	−0.02	0.04	−0.02	0.01
CP-5,21-H	−7.89	−1.91	2.08	6.14
***opp*-DCP-21,23-H**	0.00	0.00	0.00	0.00
***opp*-DCP-21,22-H**	3.84	−7.78	4.32	0.22
***opp*-DCP-22,24-H**	13.62	−13.63	13.70	−13.70
***opp*-DCP-5,22-H**	4.87	−11.87	27.02	−14.97
***opp*-DCP-5,24-H**	7.73	−6.80	12.97	−13.74
***adj*-DCP-23,24-H**	−22.14	15.84	−9.05	16.00
***adj*-DCP-21,24-H**	3.68	−4.63	−0.20	1.65
***adj*-DCP-21,22-H**	0.00	0.00	0.00	0.00
***adj*-DCP-21,23-H**	7.78	−11.03	1.61	2.66
***adj*-DCP-5,23-H**	−28.43	12.20	−2.37	13.33
***adj*-DCP-10,23-H**	31.85	−17.11	−1.80	−13.68
***adj*-DCP-10,24-H**	−26.04	15.08	−1.73	13.86
***adj*-DCP-15,23-H**	−23.45	14.23	−2.14	12.90
TCP-22,24-H	−5.52	5.52	−13.96	13.96
TCP-21,23-H	−4.39	4.41	1.65	−1.64
TCP-21,24-H	−10.50	22.53	−13.74	0.41
TCP-21,22-H	0.05	−0.05	0.00	−0.01
TCP-5,23-H	−9.52	25.14	−10.00	−1.73
TCP-15,22-H	0.00	0.08	−0.14	0.06
TCP-15,24-H	26.54	−32.92	29.13	−19.13
TCP-5,24-H	28.29	−32.42	17.68	−17.77
Q-21,23-H	−2.83	2.82	2.82	−2.83
Q-21,22-H	−6.12	−8.10	19.91	8.02
Q-4,5-H	−31.76	28.50	−50.81	30.21
Q-5,21-H	25.93	−2.77	9.43	−33.04
Q-5,23-H	26.46	−6.53	6.42	−30.36
Q-1,5-H	25.39	18.97	−34.62	−29.68
Q-1,15-H	−43.35	6.15	−19.01	27.66
Q-1,10-H	−47.94	24.02	−37.56	35.65
3	−28.75	28.75	−28.75	28.75

theoretical studies.[40] **P-21,22-H** was shown to be 8.01 kcal/mol higher in energy, while the isoporphyrin structures **P-5,21-H** and **P-10,21-H** were over 40 kcal/mol higher in energy (Table 3). These results are again in accord with expectations. For the monocarbaporphyrin series, tautomer **CP-22,24-H** is lowest in energy in agreement with experimental results (Table 4). However, tautomer **CP-21,23** is only approximately 3 kcal/mol higher in energy, and this indicates that structures with internal CH_2 units are quite accessible. Interestingly, palladium(II) complexes of this tautomer have been reported recently.[28,29] **CP-22,23-H** is 6 kcal/mol higher than **CP-22,24-H** due to the proximity of the NH protons (Table 4). Although there are

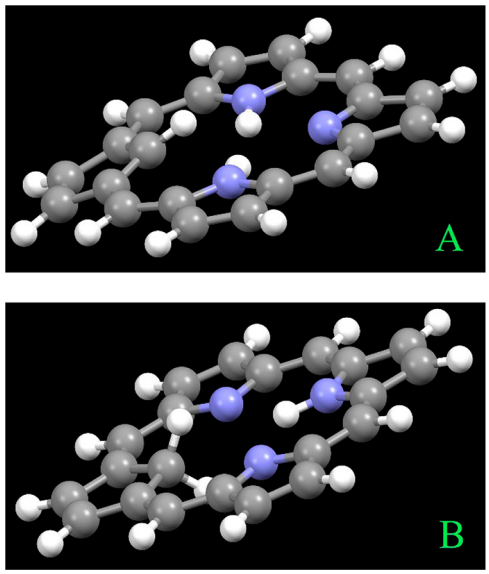

Figure 1. Mercury 3.1 rendering of the minimized conformations of monocarbaporphyrins **CP-22,24-H** (A) and **CP-21,23-H** (B).

three adjacent hydrogens within the cavity in both cases, the lower energy tautomer allows for effective hydrogen-bonding interactions. Tautomer **CP-21,22-H** also has an 18-π-electron delocalization pathway, but this is nearly 10 kcal/mol higher in energy. This can be attributed to reduced hydrogen-bonding interactions and increased pyrrolenine lone pair−lone pair repulsion. Isocarbaporphyrins **CP-5,23-H**, **CP-5,22-H**, **CP-5,24-H**, **CP-10,23-H**, **CP-10,24-H**, and **CP-10,22-H** all have a break in the conjugation pathway and as a result have calculated energies of between 24.19 and 32.13 kcal/mol higher than **CP-22,24-H**. Within this subgroup, the higher energy structures have less effective hydrogen-bonding interactions. Structures **CP-10,21-H** and **CP-5,21-H** both have an internal CH_2 and a methylene bridge and unsurprisingly are approximately 50 kcal/mol higher in energy (Table 4).

The diatropicities of the tautomers were assessed using nucleus-independent chemical shifts (NICSs).[41] The NICS allows the magnetic shielding at ring centers to be computed, and a strongly negative value is considered to be a criterion for aromatic character.[41] Although NICS calculations can sometimes give misleading results,[42] they have been widely applied to porphyrinoid systems and the matched set of structures assessed in this paper appears to give meaningful results. NICSs were calculated for the center of the macrocycle, for 1.00 Å above the mean macrocyclic plane, and for the individual five-membered rings. For the porphyrin tautomers **P-21,23-H** and **P-21,22-H**, the central NICS values were calculated as −14.87 and −14.38, respectively (Table 3). The values for 1.00 Å above the plane were slightly lower. The pyrrole-type ring (labeled as *a*) gave values of −12.33 and −12.65 for these two structures, while the pyrrolenine rings, which can be considered to be components of azafulvene units, gave much lower values. It is important to note that the center of ring *a* lies within the 18-π-electron delocalization pathway, while the center of ring *b* is outside of the pathway. Therefore, the macrocyclic ring current and the 6-π-electron current for ring *a* reinforce one another, while the opposite is the case for ring *b*. In the isoporphyrin structures **P-5,21-H** and **P-10,21-H**, the central position gave a negligible value of less than −3 (Table 3). Only the pyrrole type ring (rings *b* and *c*, respectively, for the two structures)

dx.doi.org/10.1021/jo4021198 | J. Org. Chem. 2013, 78, 11535−11548

Table 2. Angles (deg) between the Plane of Each of the Five-Membered Rings and the Overall Plane of the Macrocycle

structure	ring *a*	ring *b*	ring *c*	ring *d*
P-21,23-H	0.00	0.00	0.00	0.00
P-21,22-H	0.02	0.02	0.02	0.02
P-5,21-H	0.04	0.05	0.03	0.04
P-10,21-H	0.46	0.21	0.11	0.19
CP-22,24-H	14.96	2.03	1.87	2.11
CP-21,23-H	0.00	0.00	0.00	0.00
CP-22,23-H	12.36	0.42	2.84	6.55
CP-21,22-H	0.00	0.00	0.00	0.00
CP-5,23-H	0.15	0.02	0.03	0.02
CP-5,22-H	9.16	5.21	0.69	1.19
CP-5,24-H	0.05	0.07	0.03	0.03
CP-10,23-H	0.31	0.23	0.18	0.10
CP-10,24-H	0.13	0.19	0.11	0.07
CP-10,22-H	0.13	0.08	0.17	0.08
CP-10,21-H	0.06	0.04	0.07	0.05
CP-5,21-H	11.14	3.88	2.00	2.54
***opp*-DCP-21,23-H**	0.00	0.00	0.00	0.00
***opp*-DCP-21,22-H**	2.01	5.23	6.31	0.70
***opp*-DCP-22,24-H**	15.49	6.16	15.50	6.26
***opp*-DCP-5,22-H**	6.18	3.50	16.75	18.88
***opp*-DCP-5,24-H**	10.50	1.07	9.79	10.18
***adj*-DCP-23,24-H**	16.17	16.35	8.46	8.77
***adj*-DCP-21,24-H**	2.78	7.08	1.10	1.28
***adj*-DCP-21,22-H**	0.00	0.00	0.00	0.00
***adj*-DCP-21,23-H**	4.69	14.66	1.47	2.61
***adj*-DCP-5,23-H**	19.24	17.75	2.36	3.13
***adj*-DCP-10,23-H**	30.30	10.87	8.21	15.40
***adj*-DCP-10,24-H**	17.45	19.42	4.11	4.38
***adj*-DCP-15,23-H**	16.52	16.72	2.60	2.53
TCP-22,24-H	15.95	5.55	15.95	5.11
TCP-21,23-H	3.34	9.22	3.33	2.16
TCP-21,24-H	2.77	17.52	14.16	6.47
TCP-21,22-H	0.02	0.08	0.04	0.04
TCP-5,23-H	3.72	19.04	13.13	2.94
TCP-15,22-H	0.13	0.10	0.23	0.04
TCP-15,24-H	18.87	21.69	26.46	15.02
TCP-5,24-H	17.57	25.10	18.92	11.18
Q-21,23-H	0.99	3.12	1.01	3.12
Q-21,22-H	2.50	2.44	13.56	13.49
Q-4,5-H	20.75	27.74	24.36	27.93
Q-5,21-H	16.32	19.96	13.33	29.58
Q-5,23-H	21.07	16.92	3.67	18.56
Q-1,5-H	17.52	15.56	66.79	23.07
Q-1,15-H	11.45	44.10	3.01	28.78
Q-1,10-H	39.43	15.16	38.44	17.12
3	20.65	20.65	20.65	20.65

showed substantial shielding (Table 3), indicating that the pyrrolenine rings exhibit relatively small ring current effects. The favored monocarbaporphyrin tautomer **CP-22,24-H** shows ring currents comparable to those of **P-21,23-H**, and the center of the macrocycle gave a value of −14.15 (Table 4). This is in good agreement with the large ring current effects observed in the proton NMR spectra of carbaporphyrins, where the internal CH is commonly observed upfield near −7 ppm. The pyrrole rings gave a value of −13.03, whereas the cyclopentadiene unit afforded a deshielded value of +5.05 and the pyrrolenine ring was calculated as −3.17. These results are similar to those obtained for porphyrin. The positive value for the cyclopentadiene ring can be attributed to the central point lying outside of the 18-π-electron delocalization pathway. However, the ring current associated with the carbocyclic ring must be far smaller than the one due to the pyrrolenine ring. **CP-21,23-H** also has a highly shielded interior and the central point was calculated as −13.31. Ring *a*, which corresponds to the cyclopentadiene ring, gave an even higher value (−16.68), and this is due to the carbon ring lying inside of the 18-π-electron delocalization pathway. The pyrrole ring (*c*) was calculated as −12.76, while the pyrrolenine ring (*b*) gave a value of −0.92, and these results are roughly comparable to the trends seen above. Tautomers **CP-22,23-H** and **CP-21,22-H**, both of which are fully conjugated structures, gave similar values that can be rationalized in the same way (Table 4). Not surprisingly, the remaining nonaromatic tautomers gave very low values for the center of the macrocycle, although the aromatic character of the pyrrole rings can still be discerned.

Dicarbaporphyrins. Porphyrinoid systems with two internal carbon atoms have been less well studied, and only one example of an *opp*-dicarbaporphyrin (**4**) has been reported to date (Scheme 1).[20] This dibenzodicarbaporphyrin proved to be somewhat unstable but exhibited a strong diamagnetic ring current, as assessed by proton NMR spectroscopy. In $CDCl_3$, the internal CHs gave rise to a 2H upfield singlet at −4.34 ppm and the NHs afforded a broad peak at −3.30 ppm. In addition, the *meso* protons were strongly deshielded and gave rise to a 4H singlet at 10 ppm.[20] Addition of TFA afforded the related *C*-protonated monocation **4**H$^+$ (Scheme 1), and this showed comparable diatropic character. In this case, the interior CH_2 and CH afforded singlets at −4.34 and −3.30 ppm, respectively, while the NH peak was observed at −0.95 ppm. The *meso* protons were similarly deshielded, giving rise to two 2H singlets at 10.02 and 10.35 ppm.[20] The UV−vis spectrum for **4** also closely resembled the spectra for porphyrins, showing a Soret band at 442 nm and a series of Q bands at higher wavelengths.[20] *adj*-Dicarbaporphyrins are not currently known, but the related dioxadicarbaporphyrin system **5** has been reported (Scheme 1).[43] Porphyrinoids **5** are far more robust and also exhibited highly diatropic character. The proton NMR spectrum for **5a** showed a 2H singlet at −4.29 ppm for the internal CH protons, while the *meso* protons gave rise to three downfield resonances at 9.15 (1H), 9.40 (2H), and 9.91 ppm (1H).[43] Addition of TFA afforded the related *C*-protonated cation **5**H$^+$ (Scheme 1), and this also retained strongly diatropic characteristics.[43] The interior CH_2 and CH now appeared at −6.08 and −4.42 ppm, respectively, while the *meso* protons gave rise to four 1H singlets at 9.47, 10.10, 10.12, and 10.47 ppm. The UV−vis spectrum for **5** was less porphyrin-like, although a Soret band was observed at 436 nm. An X-ray crystal structure of phenyl-substituted dioxadicarbaporphyrin **5b** was also obtained, and this showed that the structure is near planar and the bond lengths are consistent with an aromatic 18-π-electron delocalized structure.[43]

Five ***opp*-DCP** and eight ***adj*-DCP** tautomers were considered in our analysis. As all 13 structures are isomeric, direct comparisons can be made between the two series of dicarbaporphyins. The macrocyclic structures were optimized, and ***opp*-DCP-21,23-H** was shown to be planar. This structure has an 18-π-electron delocalization pathway but possesses two internal CH_2 units. Even though the macrocyclic cavity is enclosed by the four hydrogens, the sp^3-hybridized carbons reduce steric interactions by placing these atoms above and below the plane. On the other hand, tautomer ***opp*-DCP-22,24-**

dx.doi.org/10.1021/jo4021198 | J. Org. Chem. 2013, 78, 11535−11548

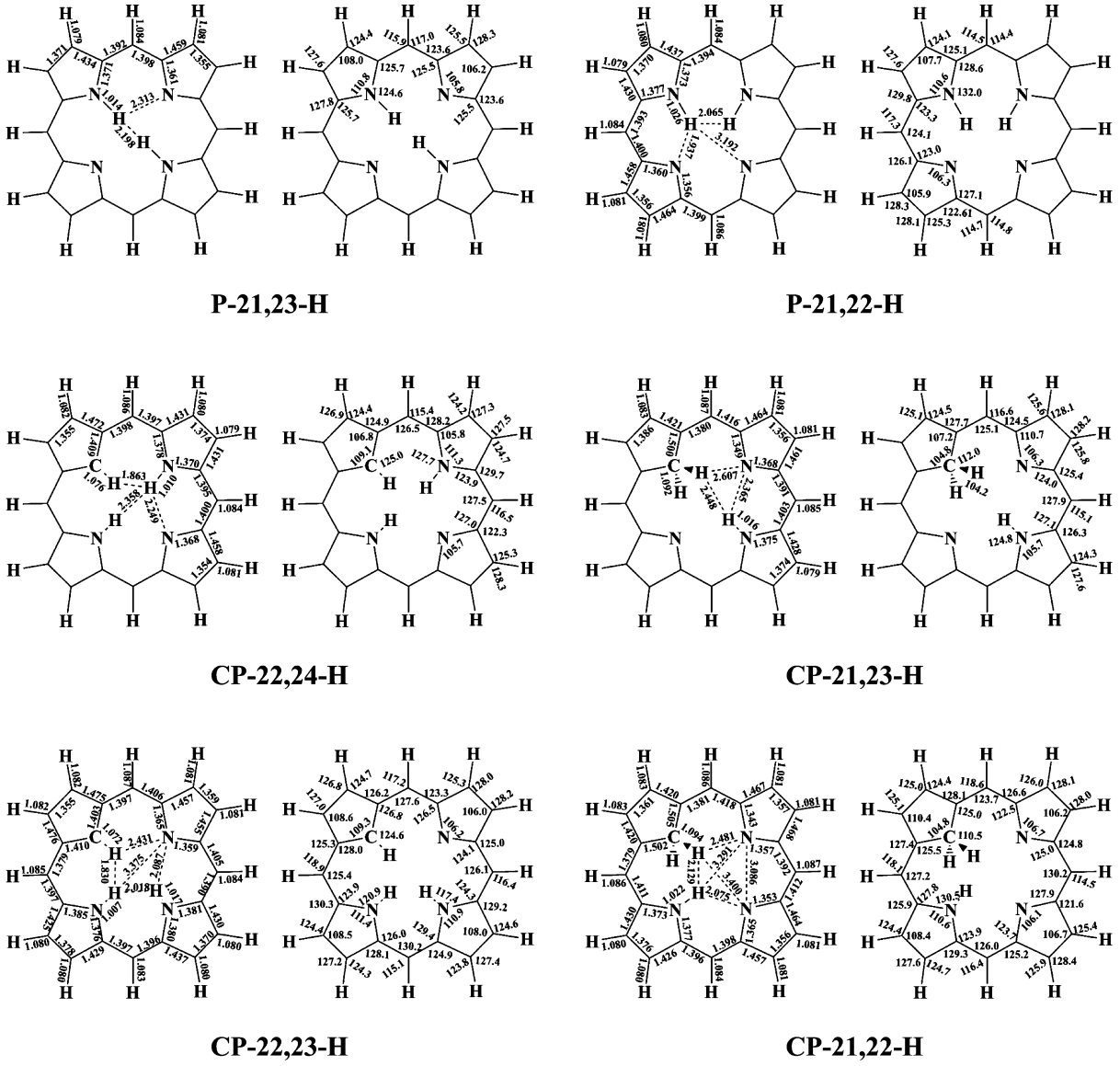

Figure 2. Bond lengths (Å) and angles (deg) for selected minimized conformations of porphyrin and monocarbaporphyrin tautomers.

Table 3. Calculated Energies (hartrees), Relative Energies (kcal/mol), and NICS Values (ppm) for Porphyrin Tautomers

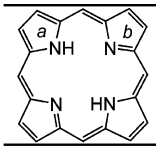	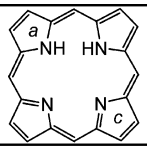	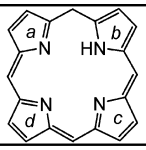	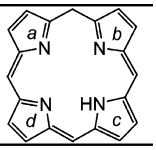
P-21,23-H	**P-21,22-H**	**P-5,21-H**	**P-10,21-H**
-989.798946	-989.786178	-989.728197	-989.732696
0	8.01	44.40	41.57
NICS(0) = -14.87	NICS(0) = -14.38	NICS(0) = -2.87	NICS(0) = -2.47
NICS(1) = -13.64	NICS(1) = -13.21	NICS(1) = -3.00	NICS(1) = -2.67
NICS(a) = -12.33	NICS(a) = -12.65	NICS(a) = -1.40	NICS(a) = +0.40
NICS(b) = -2.33	NICS(c) = -1.92	NICS(b) = -9.73	NICS(b) = -0.92
		NICS(c) = -2.40	NICS(c) = -9.21
		NICS(d) = -0.22	NICS(d) = -1.27

H, which is equivalent to the known dibenzoporphyrinoid **4**, is quite distorted and the two cyclopentadiene rings are tilted out of the macrocyclic plane by over 15° (Figure 3 and Table 2). The two pyrrole rings are also slightly rotated by a little over 6° (Table 2). ***opp*-DCP-21,22-H**, which has intermediary features, shows some distortion, but in this case the carbon ring is only rotated by a little over 5° relative to the macrocyclic plane. The nonaromatic isoporphyrin analogues ***opp*-DCP-5,22-H** and ***opp*-DCP-5,24-H** are also distinctly nonplanar (Tables 1 and 2). In the *adj*-dicarbaporphyrin series, the tautomer ***adj*-DCP-21,22-H** was calculated to be planar. This aromatic structure possesses two internal methylene units that alleviate strain by placing the hydrogens above and below the plane of the macrocycle. Nevertheless, the closer proximity of these units makes this result a little surprising. The more conventional tautomer ***adj*-DCP-23,24-H** is far more crowded, and a planar conformation would have to accommodate four internal hydrogens. For this reason, the cyclopentadiene rings are rotated by more than 16°, while the pyrrole rings are pivoted by >6° (Figure 3). Tautomer ***adj*-DCP-21,24-H** has an intermediary structure with an interior CH and CH_2 unit where the NH is next to the methylene group, and as expected this system shows less distortion. In this case, one of the cyclopentadiene rings is tilted by 7.08°, but the second carbocyclic unit is only rotated by <3° (Figure 3). The related tautomer ***adj*-DCP-21,23-H** differs by having the NH next to the internal CH, and

dx.doi.org/10.1021/jo4021198 | J. Org. Chem. 2013, 78, 11535−11548

Table 4. Calculated Energies (hartrees), Relative Energies (kcal/mol), and NICS Values (ppm) for Monocarbaporphyrin Tautomers

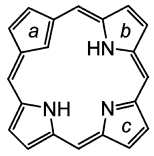	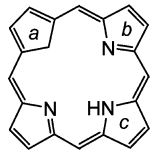	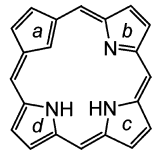	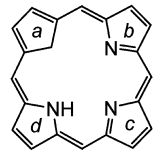	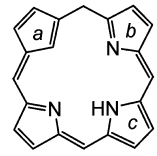	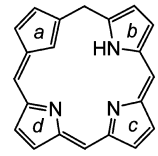
CP-22,24-H	**CP-21,23-H**	**CP-22,23-H**	**CP-21,22-H**	**CP-5,23-H**	**CP-5,22-H**
-973.722165	-973.717409	-973.712594	-973.706641	-973.683617	-973.670967
0	2.98	6.01	9.74	24.19	32.13
NICS(0) = -14.15	NICS(0) = -13.31	NICS(0) = -13.29	NICS(0) = -13.33	NICS(0) = -2.24	NICS(0) = -2.36
NICS(1) = -13.38	NICS(1) = -12.47	NICS(1) = -12.53	NICS(1) = -12.36	NICS(1) = -2.27	NICS(1) = -2.56
NICS(a) = +5.05	NICS(a) = -16.68	NICS(a) = +7.79	NICS(a) = -17.08	NICS(a) = +6.83	NICS(a) = +4.55
NICS(b) = -13.03	NICS(b) = -0.92	NICS(b) = -3.27	NICS(b) = +0.43	NICS(b) = -1.33	NICS(b) = -9.70
NICS(c) = -3.17	NICS(c) = -12.76	NICS(c) = -12.55	NICS(c) = -1.97	NICS(c) = -9.41	NICS(c) = -3.00
		NISC(d) = -14.20	NISC(d) = -13.10	NISC(d) = -1.76	NISC(d) = -0.74

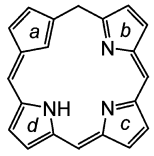	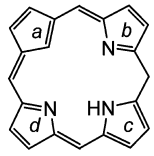	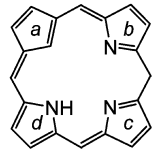	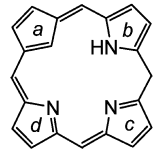	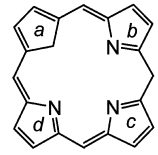	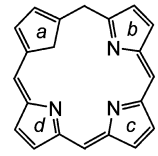
CP-5,24-H	**CP-10,23-H**	**CP-10,24-H**	**CP-10,22-H**	**CP-10,21-H**	**CP-5,21-H**
-973.676433	-973.682545	-973.677018	-973.675544	-973.643617	-973.636685
28.70	24.86	28.33	29.26	49.29	53.64
NICS(0) = -2.18	NICS(0) = -1.96	NICS(0) = -2.29	NICS(0) = -2.06	NICS(0) = -3.04	NICS(0) = -2.20
NICS(1) = -2.23	NICS(1) = -2.08	NICS(1) = -2.31	NICS(1) = -2.14	NICS(1) = -3.28	NICS(1) = -2.30
NICS(a) = +5.15	NICS(a) = +5.63	NICS(a) = +4.45	NICS(a) = +2.69	NICS(a) = +5.00	NICS(a) = -4.25
NICS(b) = -0.14	NICS(b) = -2.69	NICS(b) = -1.16	NICS(b) = -10.46	NICS(b) = -0.01	NICS(b) = -0.57
NICS(c) = -2.27	NICS(c) = -9.84	NICS(c) = -1.56	NICS(c) = -2.38	NICS(c) = +0.47	NICS(c) = +0.04
NICS(d) = -9.27	NICS(d) = -3.55	NICS(d) = -9.81	NICS(d) = -2.30	NICS(d) = +0.09	NICS(d) = -1.53

Scheme 1

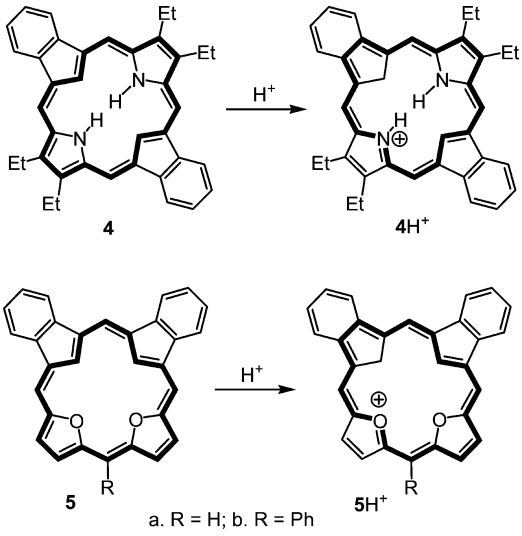

this results in much larger distortions. The cyclopentadiene units are tilted by 4.69 and 14.6°, although the pyrrole moieties are only slightly rotated relative to the mean macrocyclic plane. The remaining tautomers are all nonaromatic and show relatively nonplanar conformations (Tables 1 and 2).

The calculated bond lengths and angles for the fully conjugated dicarbaporphyrin tautomers are shown in Figure 4. The values for ***opp*-DCP-22,24-H** and ***adj*-DCP-23,24-H** are in reasonable agreement with the results reported by Feng and co-workers. Although a degree of bond length alternation is present in the fully conjugated structures, the results are consistent with porphyrin-like aromatic systems. The assessment of steric crowding within the cavity was again insightful. ***opp*-DCP-22,24-H** has four inner hydrogens, and the CH to NH distance is only 1.948 Å (Figure 4), even though this is a nonplanar structure (Figure 3). In ***opp*-DCP-21,23-H**, which is a planar structure with two internal CH_2 units, the CH−CH separation is a very reasonable 2.396 Å, but tautomer ***opp*-DCP-21,22-H** with a single inner methylene group has a CH and an NH forced to lie 1.756 Å apart (Figure 4). In ***adj*-DCP-23,24-H**, which has four inner hydrogens, the CH−NH distance is 2.006 Å and the CH−CH distance is 2.005 Å. Tautomer ***adj*-DCP-21,22-H**, which has two internal methylene units present, has a CH−CH distance of 2.001 Å, which does little to relieve steric crowding. Two of the fully conjugated *adj*-dicarbaporphyrin tautomers have a single CH_2 unit. The tautomer ***adj*-DCP-21,23-H** has internal CH−CH_2 separations of 2.136 Å and the NH−CH separation is 1.864 Å. However, in ***adj*-DCP-21,24-H**, the closest CH−NH distance is 2.050 Å and the CH−CH_2 distance is 2.039 Å. There is something of a tradeoff in the bond distances, although the CH−NH separation is improved in the latter species.

The relative energies of the tautomers were calculated, and these allowed the two series to be compared and contrasted (Table 5). In the *opp*-dicarbaporphyrin series, tautomer ***opp*-DCP-22,24-H** is lowest in energy. As this corresponds to the known dibenzodicarbaporphyrin **4**, this result is supported by the available experimental evidence. However, ***opp*-DCP-21,22-H** with an interior CH_2 is only 2.47 kcal/mol higher in energy, and even ***opp*-DCP-21,23-H** is only 6.38 kcal/mol higher than the low-energy tautomer (Table 5). These results indicate that these tautomers should all be accessible. However, the nonaromatic tautomers ***opp*-DCP-5,22-H** and ***opp*-DCP-5,24-**

dx.doi.org/10.1021/jo4021198 | J. Org. Chem. 2013, 78, 11535−11548

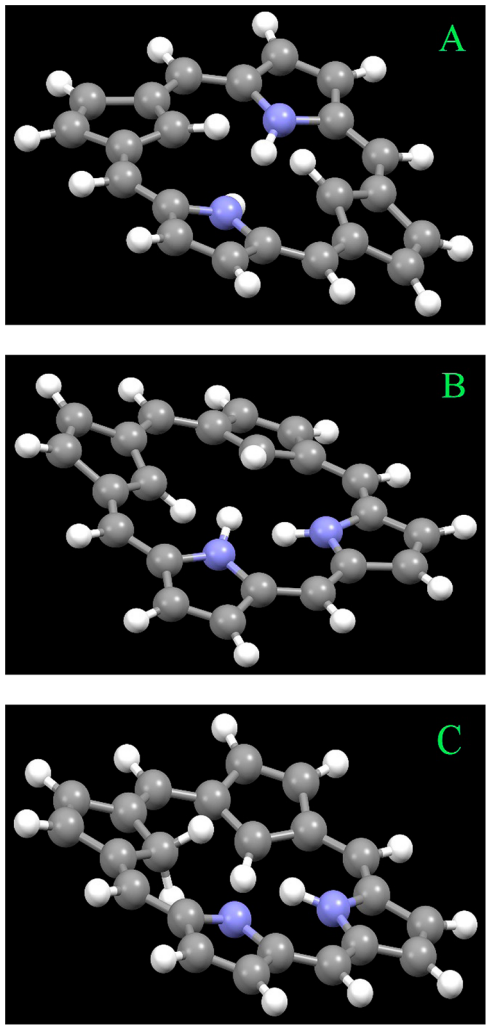

Figure 3. Mercury 3.1 rendering of the minimized conformations of dicarbaporphyrins ***opp*-DCP-22,24-H** (A), ***adj*-DCP-23,24-H** (B), and ***adj*-DCP-21,23-H** (C).

H are both approximately 20 kcal/mol higher in energy. In the *adj*-dicarbaporphyrin series, none of the tautomers are as low in energy as ***opp*-DCP-22,24-H**. Counterintuitively, the lowest energy form ***adj*-DCP-21,23-H** has an internal methylene unit, but this is still 0.54 kcal/mol higher in energy than ***opp*-DCP-22,24-H**. The related form ***adj*-DCP-21,24-H**, where the NH is adjacent to the CH, is just over 1 kcal/mol higher in energy. The expected structure ***adj*-DCP-23,24-H** is 4.78 kcal/mol higher in energy, but this is still an accessible species. Predictably, the nonaromatic structures were much higher in energy and therefore of limited significance (Table 5). NICS calculations showed that all of the continuously conjugated tautomers are highly diatropic (Table 5). Hence, the favored *opp*-dicarbaporphyrin tautomer gave a NICS value for the middle of the macrocycle of −13.81. Although the individual pyrrole rings gave a value of −13.77, the cyclopentadiene gave a small positive value of +3.94. Again, this makes sense because the center of the cyclopentadiene ring lies outside of the 18-π-electron delocalization pathway. In tautomer ***opp*-DCP-21,22-H**, the macrocycle gave a value of −12.02 and the pyrrole gave an even higher value of −14.04. In one cyclopentadiene unit (ring *a*) the center lies within the 18-π-electron delocalization pathway and consequently gives a value of −15.09, but the center of ring *c* lies outside of the pathway and gives a NICS value of +7.31. Tautomer ***opp*-DCP-21,23-H**, with two internal methylenes, has a macrocyclic value of −13.94 and the cyclopentadiene units give a higher value of −17.45. Again, the center of these cyclopentadiene rings lies inside the macrocyclic pathway. The pyrrolenine rings gave values of +0.81 due to the center of these rings lying outside of the [18]annulene pathway (Table 5). Similar results were obtained for the fully conjugated structures in the *adj*-dicarbaporphyrin series. As would be expected, the nonaromatic structures in both series gave very small values for the macrocycle and only the pyrrole rings gave significant results that correspond to aromatic species (Table 5).

Tricarbaporphyrins and Quatyrins. As the number of carbon atoms increases, the number of hydrogens that must be placed within the macrocyclic cavity also gets larger. This is a greater problem for the aromatic species than for the nonaromatic versions, and it was not clear to us whether this factor might lower the stability of the aromatic forms relative to the nonaromatic versions. Eight tautomers of tricarbaporphyrin and another eight tautomers of quatyrin were considered. Of these structures, only quatyrin **Q-21,23-H** has been calculated previously,[39] and very few details were provided in that study. In fact, quatyrin was only considered for comparison to the tetraoxaporphyrin dication, and little information apart from calculated bond lengths and angles was provided in this analysis.[39] In the aromatic forms of tricarbaporphyrin, at least one internal methylene unit must be present, while the aromatic versions of quatyrin have to have two interior CH_2 units. The macrocyclic structures were optimized using the previous methods. In the tricarbaporphyrin series, **TCP-21,22-H** was shown to be near planar, even though five hydrogens are present within the cavity and two methylene units are adjacent to one another (Tables 1 and 2). The more conventional structure **TCP-22,24** has one inner CH_2 and an NH, but steric interactions with the remaining internal CHs causes significant distortions and the cyclopentadiene rings are tilted nearly 16° from the mean macrocyclic plane (Figure 5). The tautomer **TCP-21,24-H** shows similar distortions but the remaining aromatic tautomer **TCP-21,23-H** with opposite CH_2 units is closer to planarity, although one of the carbocyclic rings is tilted from the macrocyclic plane by 9.22°. The nonaromatic tautomer **TCP-15,22-H** is surprisingly planar, but the remaining tautomers **TCP-5,23-H**, **TCP-15,24-H**, and **TCP-5,24-H** are decidedly nonplanar. The calculated bond lengths and angles for the fully conjugated tricarbaporphyrin tautomers are shown in Figure 6. Again, some bond length alternation is present but the data for these fully conjugated structures are consistent with aromatic species. The favored tautomer **TCP-22,24-H** has five internal hydrogens, and the CH−CH_2 separations are 2.101 Å, while the NH−CH distance is 1.941 Å. **TCP-21,23-H** has two internal methylene groups, and this relieves crowding, as the CH−CH_2 separation is 2.041 Å.

TCP-22,24-H has the NH next to the methylene unit, and the interior CH−CH bond separation is 2.087 Å, the CH−CH_2 separation is 1.999 Å, the NH−CH_2 distance is 2.057 Å, and the CH−NH distance is only 1.913 Å. Finally, **TCP-21,22-H** has two adjacent internal methylene units and the hydrogen−hydrogen separation for between the CH_2 groups is 1.994 Å, while the CH−CH_2 distance is 2.012 Å (Figure 6).

In the quatyrin series, **Q-21,23-H** is fairly planar and the cyclopentadiene rings are only tilted relative to the mean macrocyclic plane by 1.01−3.12° (Figure 5 and Table 2). In

dx.doi.org/10.1021/jo4021198 | J. Org. Chem. 2013, 78, 11535−11548

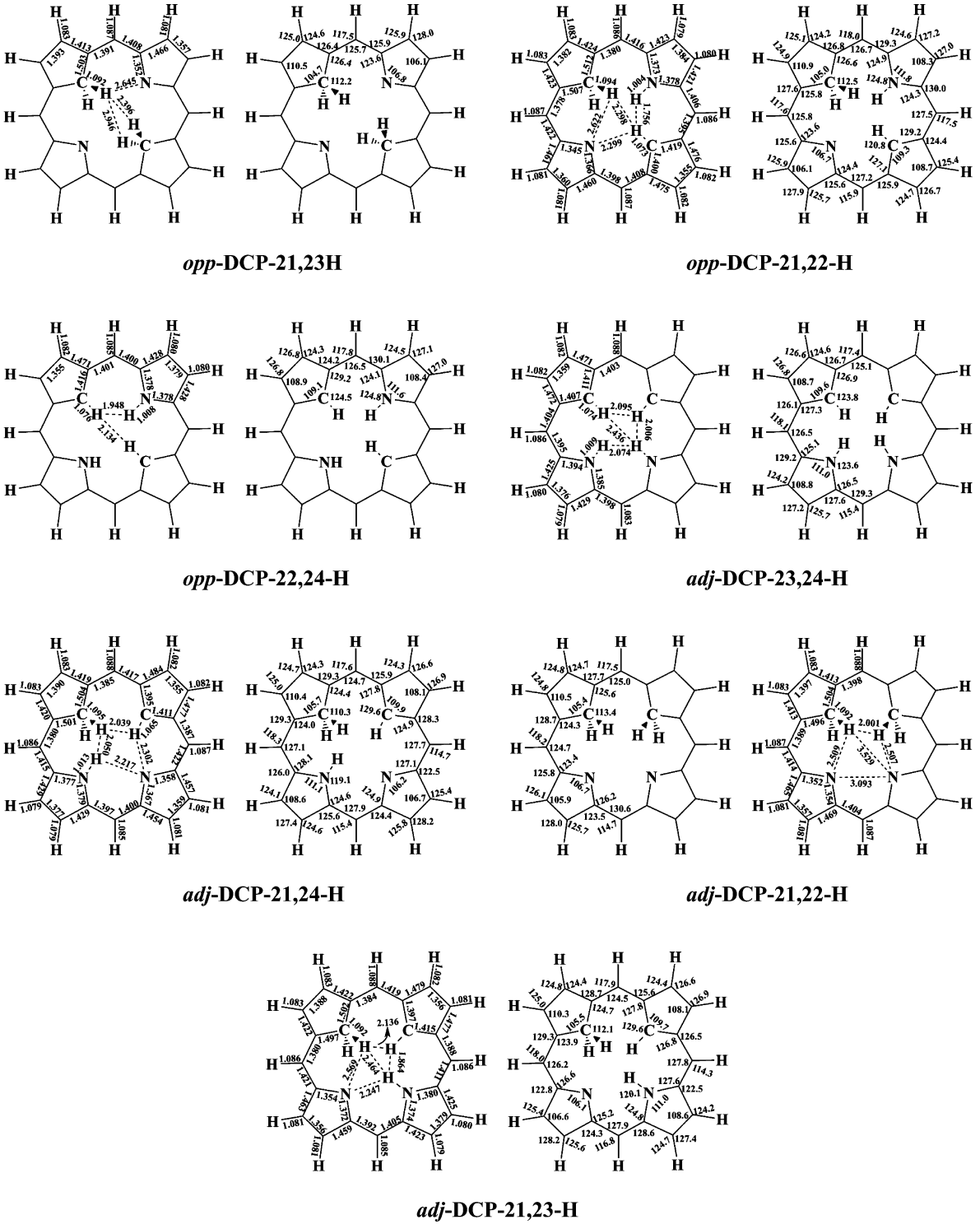

Figure 4. Bond lengths (Å) and angles (deg) for selected minimized conformations of dicarbaporphyrin tautomers.

isoquatyrin (**Q-21,22-H**), the two inner methylene groups are placed next to one another and this results in two of the carbocyclic rings being tilted from the mean macrocyclic plane by over 13° (Figure 5). The calculated bond lengths and angles for **Q-21,23-H** and **Q-21,22-H** are shown in Figure 6. These results are fully consistent with the presence of fully delocalized bridged [18]annulene structures. The double bonds lying outside of this pathway have shorter bond lengths (1.356 and 1.358 Å, respectively) that are consistent with olefinic units, while the bonds connecting these units to the [18]annulene moiety are 1.480 and 1.476 Å, respectively, which suggests that these are carbon−carbon single bonds. **Q-21,23-H** and **Q-21,22-H** have six inner hydrogens, but these are reasonably far apart. In quatyrin **Q-21,23-H**, the methylene group hydrogen to hydrogen separation is 2.813 Å, while the C−H to CH_2 separation is 1.937 Å. For isoquatyrin (**Q-21,22-H**), these separations are 2.039 and 2.203 Å, respectively. Hence, the difference in steric crowding between these two isomers is minimal. The remaining six tautomers of quatyrin, all of which lack a macrocyclic delocalization pathway, are somewhat

dx.doi.org/10.1021/jo4021198 | J. Org. Chem. 2013, 78, 11535−11548

Table 5. Calculated Energies (hartrees), Relative Energies (kcal/mol), and NICS Values (ppm) for *opp*- and *adj*-Dicarbaporphyrin Tautomers

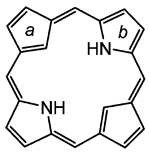	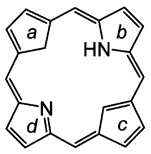	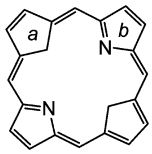	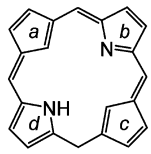	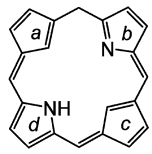
***opp*-DCP-22,24-H**	***opp*-DCP-21,22-H**	***opp*-DCP-21,23-H**	***opp*-DCP-5,22-H**	***opp*-DCP-5,24-H**
-957.645109	-957.641174	-957.634940	-957.611691	-957.613472
0	2.47	6.38	20.97	19.85
NICS (0) = -13.81	NICS (0) = -12.02	NICS (0) = -13.94	NICS (0) = -1.45	NICS (0) = -1.45
NICS (1) = -13.27	NICS (1) = -11.23	NICS (1) = -13.13	NICS (1) = -1.55	NICS (1) = -1.50
NICS (a) = +3.94	NICS (a) = -15.09	NICS (a) = -17.45	NICS (a) = +0.96	NICS (a) = +2.36
NICS (b) = -13.77	NICS (b) = -14.04	NICS (b) = +0.81	NICS (b) = -1.96	NICS (b) = -2.03
	NICS (c) = +7.31		NICS (c) = +2.18	NICS (c) = +1.18
	NICS (d) = -1.53		NICS (d) = -10.55	NICS (d) = -11.19

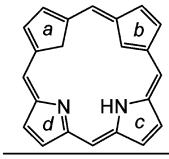	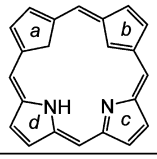	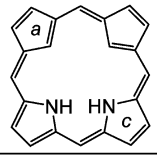	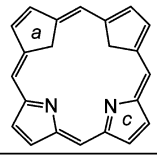
***adj*-DCP-21,23-H**	***adj*-DCP-21,24-H**	***adj*-DCP-23,24-H**	***adj*-DCP-21,22-H**
-957.644255	-957.642471	-957.636633	-957.621903
0.54	1.66	5.32	14.56
NICS (0) = -12.44	NICS (0) = -12.30	NICS (0) = -11.30	NICS (0) = -13.63
NICS (1) = -11.09	NICS (1) = -11.19	NICS (1) = -10.82	NICS (1) = -12.76
NICS (a) = -15.73	NICS (a) = -16.09	NICS (a) = +4.78	NICS (a) = -17.73
NICS (b) = +7.29	NICS (b) = +11.05	NICS (c) = -13.39	NICS (c) = +0.69
NICS (c) = -13.44	NICS (c) = -3.76		
NICS (d) = -1.97	NICS (d) = -13.08		

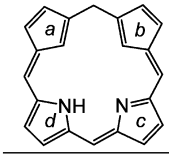	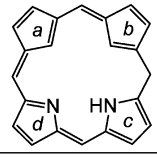	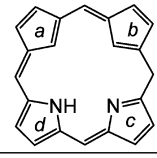	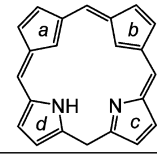
***adj*-DCP-5,23-H**	***adj*-DCP-10,23-H**	***adj*-DCP-10,24-H**	***adj*-DCP-15,23-H**
-957.616173	-957.615346	-957.616772	-957.616843
18.16	18.68	17.78	17.73
NICS (0) = -1.07	NICS (0) = +1.24	NICS (0) = -0.45	NICS (0) = -0.74
NICS (1) = -1.40	NICS (1) = +1.12	NICS (1) = -0.99	NICS (1) = -1.26
NICS (a) = +1.79	NICS (a) = +1.14	NICS (a) = +2.39	NICS (a) = +0.15
NICS (b) = +3.50	NICS (b) = -1.37	NICS (b) = +2.40	NICS (b) = +1.60
NICS (c) = -3.33	NICS (c) = -9.77	NICS (c) = -1.37	NICS (c) = -3.29
NICS (d) = -10.57	NICS (d) = -4.85	NICS (d) = -9.54	NICS (d) = -10.34

nonplanar and the cyclopentadiene rings are rotated relative to the mean macrocyclic plane by up to 44°.

The relative energies of tricarbaporphyrin and quatyrin tautomers were calculated (Tables 6 and 7), and this allowed the stabilities of the aromatic and nonaromatic forms to be contrasted. In the tricarbaporphyrin series, tautomer **TCP-22,24-H** is lowest in energy and this structure has the inner CH_2 opposite to the pyrrolic NH. Tautomer **TCP-21,24-H**, which has the NH next to the CH_2 unit, is only 0.69 kcal/mol higher in energy and tautomer **TCP-21,23-H** with two internal methylene units is just 3.42 kcal/mol higher than **TCP-22,24-H** (Table 6). When the two internal CH_2 units are adjacent rather than opposite, as is the case for **TCP-21,22-H**, the energy is raised to 4.38 kcal/mol relative to the most stable tautomer. Hence, all four structures are remarkable close in energy. However, the four nonaromatic isotricarbaporphyrin tautomers are much higher in energy and range from 14.01 to 23.56 kcal/mol higher than **TCP-22,24-H** (Table 6). Nevertheless, these are energetically sufficiently close to be reasonably accessible species. Quatyrin **Q-21,23-H** is the most stable tautomer in the tetracarbaporphyrin series, although isoquatyrin (**Q-21,22-H**) is only 0.24 kcal/mol higher in energy (Table 7). The presence of two adjacent methylene units apparently causes virtually no destabilization to the structure. All of the nonaromatic species are significantly higher in energy. The isoporphyrin analogues **Q-4,5-H**, **Q-5,21-H**, **Q-5,23-H**, and **Q-1,5-H** are between 16.27 and 28.60 kcal/mol higher in energy than the aromatic quatyrin **Q-21,23-H**. Tautomers **Q-1,15-H** and **Q-1,10-H**, possessing a sp^3 carbon within the cyclopentadiene ring that is linked to a *meso* carbon, are even further destabilized with calculated energies 33.05 and 35.95 kcal/mol higher than that of the favored tautomer (Table 7).

dx.doi.org/10.1021/jo4021198 | J. Org. Chem. 2013, 78, 11535−11548

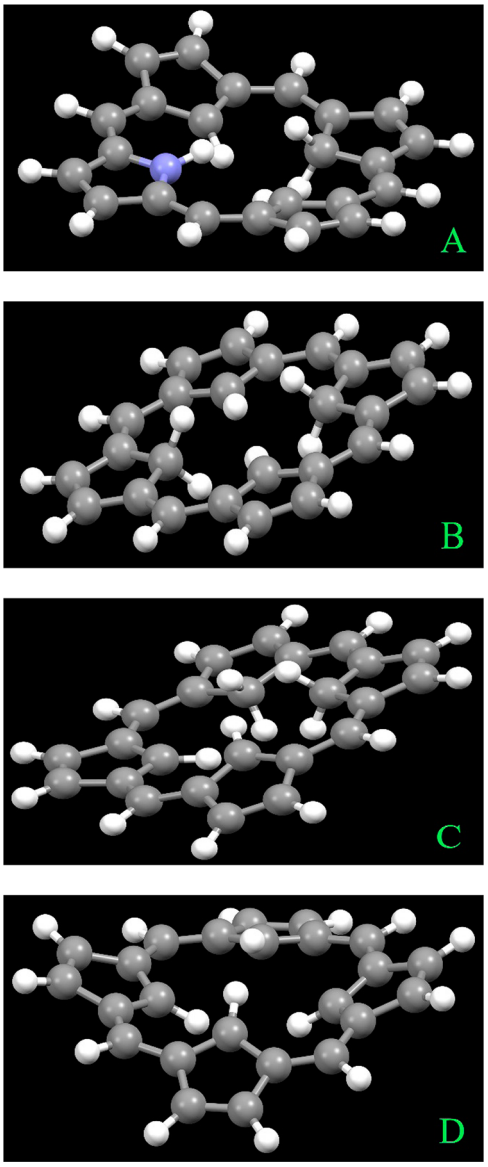

Figure 5. Mercury 3.1 rendering of the minimized conformations of tricarbaporphyrin **TCP-22,24-H** (A), quatyrin **Q-21,23-H** (B), isoquatyrin **Q-21,22-H** (C), and didehydroquatyrin **3** (D).

NICS calculations show that fully conjugated tricarbaporphyrins and quatyrins retain highly diatropic characteristics. The low-energy tricarbaporphyrin tautomer **TCP-22,24-H** gave an NICS value for the center of the macrocycle of −12.02, and the remaining pyrrole ring gave a slightly higher value of −14.21 (Table 6). The cyclopentadiene ring with an internal CH_2 gave a NICS value of −14.48, but the remaining carbocyclic ring gave a calculated value of +5.15. These results are all consistent with the trends observed for the mono- and dicarbaporphyrin series. The remaining aromatic tautomers **TCP-21,23-H**, **TCP-21,24-H**, and **TCP-21,22-H** gave similar results, and the calculated macrocyclic NICS values are −13.37, −10.11, and −12.80, respectively (Table 6). The nonaromatic forms again gave negligible NICS values for the center of the macrocycle, although some of the cyclopentadiene units gave surprisingly high positive values for the isoporphyrin analogues **TCP-5,23-H** and **TCP-15,22-H** (Table 6). This may be due to these rings taking on antiaromatic character due to dipolar resonance contributors such as **6** (Scheme 2). Quatyrin **Q-21,23-H** gave a macrocyclic NICS value of −13.05, and the cyclopentadiene rings lying within the [18]annulene delocalization pathway gave a calculated value of −16.62 (Table 7). This compares to values of −11.53 and −15.23, respectively, for isoquatyrin (**Q-21,22-H**) (Table 7). For the cyclopentadiene rings lying outside of the 18-π-electron delocalization pathway, values of +10.07 and +7.11 were obtained. This emphasizes the importance of the [18]annulene substructure in determining the aromaticity of these macrocycles. The remaining tautomers showed no significant NICS values, as would be expected for these nonaromatic structures (Table 7).

The didehydroquatyrin structure **3** was also considered. This antiaromatic system is not a known compound, but related tetracationic structures have been synthesized. Oxidation of calix[4]azulenes **7** with DDQ afforded tetraazuliporphyrin tetracations **8** (Scheme 3).[44] Computational studies indicated that these structures were highly distorted, due to steric interactions between the aryl substituents and the azulene rings, and while this system can be written as a didehydroquatyrin with four fused tropylium units (resonance contributor **8′**), the spectroscopic data indicate that there is essentially no macrocyclic conjugation. The optimized structure for **3** was nonplanar, with all four cyclopentadiene rings tilted by >20° relative to the mean macrocyclic plane due to the presence of four internal hydrogen atoms (Table 2 and Figure 5). The NICS calculations gave a value of +7.57 for the midpoint in the macrocycle, which is consistent with a paratropic species. The individual cyclopentadiene rings gave a value of −6.24, which is due to the center of the carbocyclic rings lying outside of the [16]annulene delocalization pathway (Table 7).

■ CONCLUSIONS AND FUTURE PROSPECTS

Computational studies allow individual porphyrinoid tautomers to be assessed and provide valuable insights into the characteristics of carbaporphyrinoid systems. Monocarbaporphyrins are well studied, but this work demonstrates for the first time that tautomers with internal CH_2 units are only slightly higher in energy than those with an internal CH. This helps to explain why this type of structure is favored for the palladium(II) complexes of carbaporphyrins. Internal methylene units are very accessible in dicarbaporphyrin systems as well, and in fact the lowest energy tautomer for the *adj*-dicarbaporphyrin series has a structure of this type. Even tautomers with two inner CH_2 groups are not that high in energy relative to the lowest energy tautomers. Aromatic tricarbaporphyrins are forced to have a CH_2 unit in this position, but there is only a minor penalty for introducing a second internal methylene unit. A very small preference was noted for having the two internal CH_2 groups opposite to one another rather than adjacent. The tetracarbaporphyrin structure quatyrin has two opposite CH_2 units, but it is only 0.24 kcal/mol lower in energy than isoquatyrin, where the methylene groups are adjacent to one another. NICS calculations show that all of the fully conjugated porphyrinoids exhibit highly diatropic character, and this characteristic is not closely related to the degree of planarity in these structures. Pyrrole rings within the macrocycle also give large negative values, and this can be attributed to the 6-π-electron ring current for the individual ring as well as the fact that the center of this ring lies within the 18-π-electron delocalization pathway. Pyrrolenine rings gave low NICS values due to the central position lying outside of the [18]annulene pathway. Cyclopentadiene rings with internal methylene units gave strongly negative values

dx.doi.org/10.1021/jo4021198 | J. Org. Chem. 2013, 78, 11535−11548

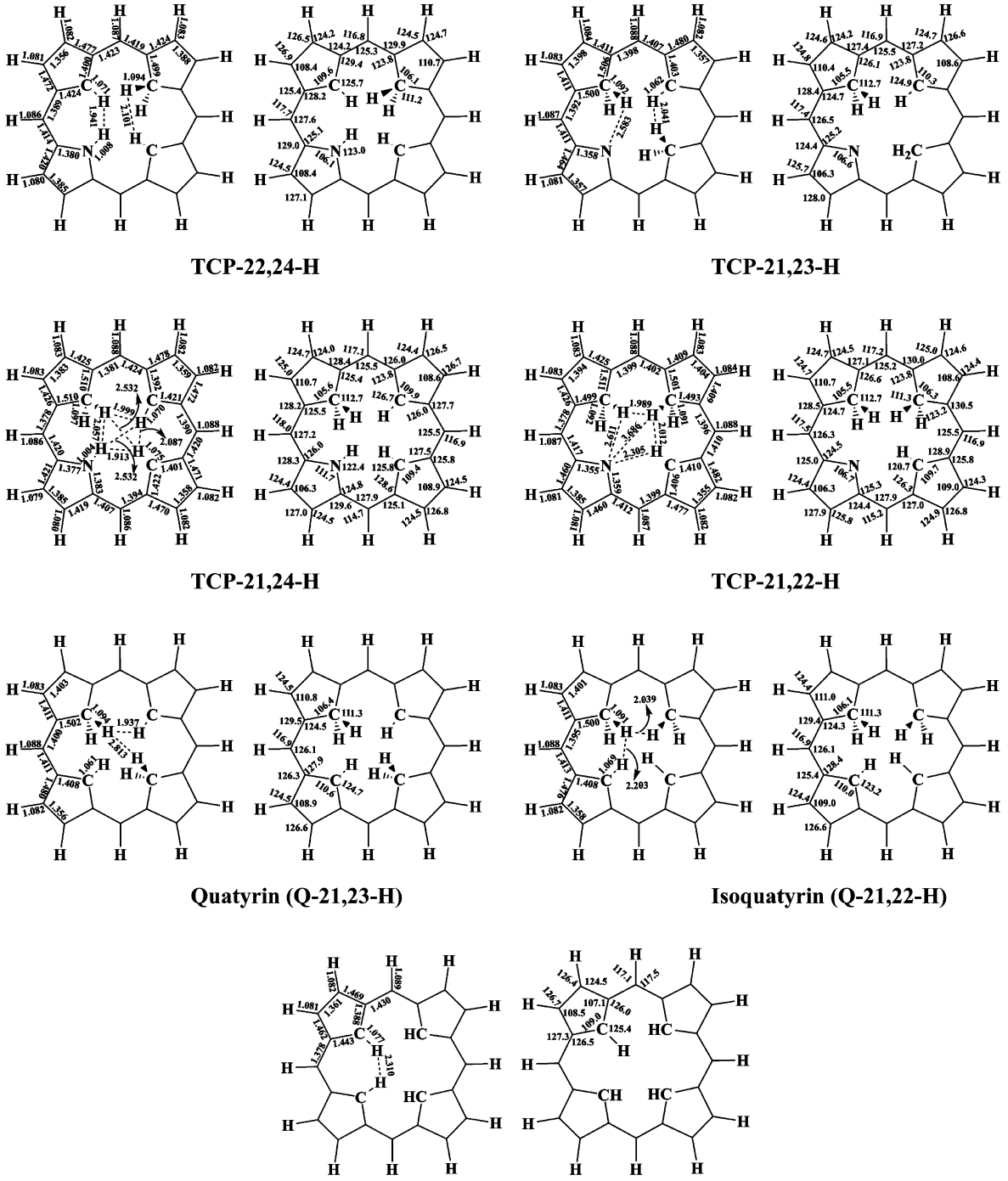

Figure 6. Bond lengths (Å) and angles (deg) for selected minimized conformations of tricarbaporphyrins, quatyrin, isoquatyrin, and didehydroquatyrin.

because the central position lies within the [18]annulene conjugation route, while cyclopentadiene moieties without an sp^3 carbon gave positive NICS values because the ring lies outside of this pathway. The results also provide a wealth of detail on the conformations, bond lengths, bond angles, and molecular orbitals for these diverse structures. Importantly, the results show that the aromatic tautomers are always strongly favored over the nonaromatic forms, even when six hydrogens are placed within the macrocyclic cavity. An increased understanding of these systems will be very helpful in designing synthetic routes to new porphyrinoid systems, including tricarbaporphyrins and quatyrins. Although it remains to be seen whether higher carbaporphyrinoid systems can be synthesized, this remains an exciting goal for future research.

■ EXPERIMENTAL SECTION

Geometry optimization calculations were performed using Spartan '10 running on a Windows platform, as provided by Wavefunction, Inc., 18401 Von Karman Ave., Suite 370, Irvine, CA 92612 (www.wavefun.com). Energy minimization calculations of the porphyrinoid systems were performed at the density functional theory (DFT) level of theory

dx.doi.org/10.1021/jo4021198 | J. Org. Chem. 2013, 78, 11535−11548

Table 6. Calculated Energies (hartrees), Relative Energies (kcal/mol), and NICS Values (ppm) for Tricarbaporphyrin Tautomers

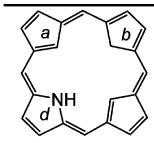	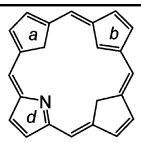	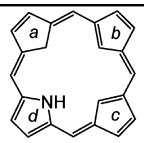	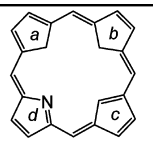
TCP-22,24-H	**TCP-21,23-H**	**TCP-21,24-H**	**TCP-21,22-H**
-941.570751	-941.565295	-941.569646	-941.563768
0	3.42	0.69	4.38
NICS (0) = -12.02	NICS (0) = -13.37	NICS (0) = -10.11	NICS (0) = -12.80
NICS (1) = -10.28	NICS (1) = -12.20	NICS (1) = -9.34	NICS (1) = -11.79
NICS (a) = +5.15	NICS (a) = -17.01	NICS (a) = -13.06	NICS (a) = -16.31
NICS (b) = -14.48	NICS (b) = +11.43	NICS (b) = +5.81	NICS (b) = -16.96
NICS (d) = -14.21	NICS (d) = -0.13	NICS (c) = +3.70	NICS (c) = +11.62
		NICS (d) = -13.60	NICS (d) = -1.78

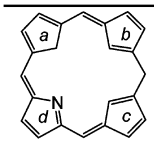	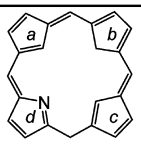	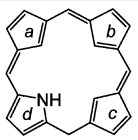	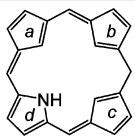
TCP-5,23-H	**TCP-15,22-H**	**TCP-15,24-H**	**TCP-5,24-H**
-941.533210	-941.533304	-941.548427	-941.548405
23.56	23.50	14.01	14.02
NICS (0) = -2.09	NICS (0) = -2.14	NICS (0) = +0.18	NICS (0) = -0.43
NICS (1) = -1.90	NICS (1) = -2.17	NICS (1) = -0.62	NICS (1) = -0.92
NICS (a) = -3.16	NICS (a) = +4.85	NICS (a) = -0.95	NICS (a) = +1.25
NICS (b) = +4.91	NICS (b) = -3.22	NICS (b) = +0.59	NICS (b) = +1.55
NICS (c) = +5.38	NICS (c) = +5.94	NICS (c) = -0.79	NICS (c) = +1.83
NICS (d) = -1.23	NICS (d) = -1.13	NICS (d) = -9.99	NICS (d) = -9.78

Scheme 2

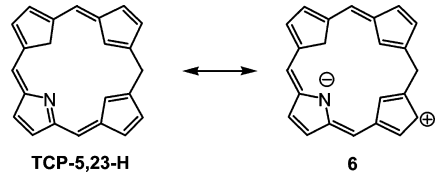

Scheme 3

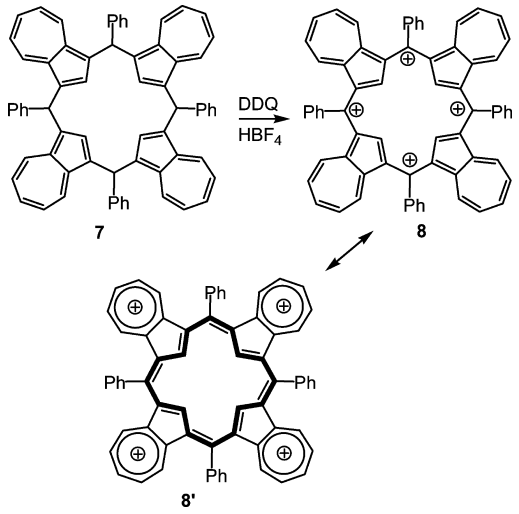

with the B3LYP functional and a 6-311++G(d,p) basis set. The SCF tolerance was set at 1×10^{-10} hartree, the gradient tolerance was set at 1×10^{-4} hartree/bohr, and the distance tolerance was set at 0.8×10^{-3}

Table 7. Calculated Energies (hartrees), Relative Energies (kcal/mol), and NICS Values (ppm) for Quatyrin Tautomers and Didehydroquatyrin 3

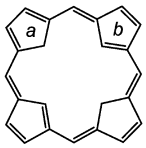	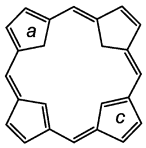	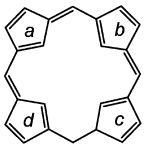	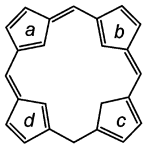	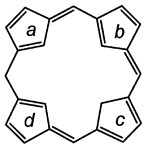
Q-21,23-H	**Q-21,22-H**	**Q-4,5-H**	**Q-5,21-H**	**Q-5,23-H**
-925.494820	-925.494438	-925.451881	-925.466426	-925.468891
0	0.24	26.94	17.82	16.27
NICS (0) = -13.05	NICS (0) = -11.53	NICS (0) = +1.55	NICS (0) = +0.83	NICS (0) = -1.35
NICS (1) = -12.18	NICS (1) = -10.54	NICS (1) = +0.59	NICS (1) = +0.96	NICS (1) = -1.75
NICS (a) = -16.62	NICS (a) = -15.23	NICS (a) = -0.00	NICS (a) = +0.04	NICS (a) = +2.20
NICS (b) = +10.07	NICS (c) = +7.11	NICS (b) = +0.18	NICS (b) = +0.31	NICS (b) = +3.32
		NICS (c) = -0.57	NICS (c) = +0.29	NICS (c) = -1.70
		NICS (d) = -1.66	NICS (d) = +0.05	NICS (d) = +3.87

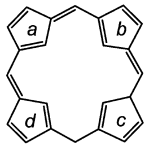	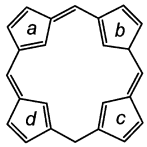	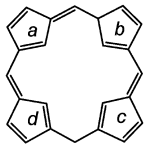	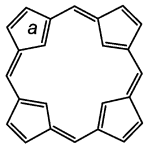
Q-1,5-H	**Q-1,15-H**	**Q-1,10-H**	**3**
-925.449249	-925.442147	-925.437524	-924.251458
28.60	33.05	35.95	---
NICS (0) = +0.35	NICS (0) = +0.32	NICS (0) = +0.46	NICS (0) = +7.57
NICS (1) = +0.29	NICS (1) = -0.30	NICS (1) = -0.13	NICS (1) = +5.69
NICS (a) = +0.66	NICS (a) = +0.47	NICS (a) = +0.56	NICS (a) = -6.24
NICS (b) = -0.48	NICS (b) = -2.12	NICS (b) = -2.28	
NICS (c) = -2.55	NICS (c) = +0.50	NICS (c) = +1.03	
NICS (d) = +0.27	NICS (d) =+0.73	NICS (d) = +1.12	

dx.doi.org/10.1021/jo4021198 | J. Org. Chem. 2013, 78, 11535−11548

angstrom. Mercury 3.1 running on an OS X platform, as provided by the CCDC (www.ccdc.cam.ac.uk/mercury/), was used to visualize the optimized structures. The resulting Cartesian coordinates of the molecules can be found in the Supporting Information. NICS calculations were performed using Gaussian 03[45] running on a Linux computer. NICS values were computed using the GIAO method,[46] at the DFT level of theory with the B3LYP functional and a 6-31+G(d,p) basis set, at several positions in each molecule. NICS(0) was calculated at the mean position of all the non-hydrogen atoms. NICS(1) was calculated 1 Å above the position of NICS(0). NICS(a), NICS(b), NICS(c), and NICS(d) values were obtained by applying the same method to the mean position of the five non-hydrogen atoms that comprise the individual rings of the macrocycle.

■ ASSOCIATED CONTENT

Supporting Information

Tables and figures giving Cartesian coordinates, Spartan '10 output summary files, and HOMO and LUMO surfaces for all of the calculated tautomers. This material is available free of charge via the Internet at http://pubs.acs.org.

■ AUTHOR INFORMATION

Corresponding Author

*E-mail for T.D.L.: tdlash@ilstu.edu.

Notes

The authors declare no competing financial interest.

■ ACKNOWLEDGMENTS

This work was supported by the National Science Foundation under Grant No. CHE-1212691, and the Petroleum Research Fund, administered by the American Chemical Society. We also thank Professor J. M. Standard for helpful discussions.

■ REFERENCES

(1) Milgrom, L. R. *The Colours of Life*; Oxford University Press: Oxford, U.K., 1997.
(2) *Handbook of Porphyrin Science-With Applications to Chemistry, Physics, Material Science, Engineering, Biology and Medicine*; Kadish, K. M., Smith, K. M., Guilard, R., Eds.; World Scientific Publishing: Singapore, 2010–2012; Vol. *1–25*.
(3) Lash, T. D. *J. Porphyrins Phthalocyanines* **2011**, *15*, 1093–1115.
(4) Vogel, E. *J. Heterocycl. Chem.* **1996**, *33*, 1461–1487.
(5) Juselius, J.; Sundholm, D. *J. Org. Chem.* **2000**, *65*, 5233–5237.
(6) Steiner, E.; Fowler, P. W. *Org. Biomol. Chem.* **2003**, *1*, 1785–1789.
(7) Steiner, E.; Fowler, P. W. *Org. Biomol. Chem.* **2004**, *2*, 34–37.
(8) Steiner, E.; Soncini, A.; Fowler, P. W. *Org. Biomol. Chem.* **2005**, *3*, 4053–4059.
(9) Steiner, E.; Fowler, P. W. *Org. Biomol. Chem.* **2006**, *4*, 2473–2476.
(10) Aihara, J.-i. *J. Phys. Chem. A* **2008**, *112*, 5305–5311.
(11) Aihara, J.-i.; Kimura, E.; Krygowski, T. M. *Bull. Chem. Soc. Jpn.* **2008**, *81*, 826–835.
(12) Aihara, J.-i.; Makino, M. *Org. Biomol. Chem.* **2010**, *8*, 261–266.
(13) Otero, N.; Fias, S.; Radenkovic, S.; Bultinck, P.; Graña, A. M.; Mandado, M. *Chem. Eur. J.* **2011**, *17*, 3274–3286.
(14) Nakagami, Y.; Sekine, R.; Aihara, J.-i. *Org. Biomol. Chem.* **2012**, *10*, 5219–5229.
(15) Aihara, J.-i.; Nakagami, Y.; Sekine, R.; Makino, M. *J. Phys. Chem. A* **2012**, *116*, 11718–11730.
(16) Wu, J. I.; Fernández, I.; Schleyer, P. v. R. *J. Am. Chem. Soc.* **2013**, *135*, 315–321.
(17) Lash, T. D. *Eur. J. Org. Chem.* **2007**, 5461–5481.
(18) Lash, T. D. In *Handbook of Porphyrin Science-With Applications to Chemistry, Physics, Material Science, Engineering, Biology and Medicine*; Kadish, K. M., Smith, K. M., Guilard, R., Eds.; World Scientific Publishing: Singapore, 2012; Vol. *16*, pp 1–329.
(19) Lash, T. D. *Synlett* **2000**, 279–295.
(20) Lash, T. D.; Romanic, J. L.; Hayes, M. J.; Spence, J. D. *Chem. Commun.* **1999**, 819–820.
(21) Berlin, K. *Angew. Chem., Int. Ed. Engl.* **1996**, *35*, 1820–1822.
(22) Lash, T. D.; Hayes, M. J.; Spence, J. D.; Muckey, M. A.; Ferrence, G. M.; Szczepura, L. F. *J. Org. Chem.* **2002**, *67*, 4860–4874.
(23) Lash, T. D.; Hayes, M. J. *Angew. Chem., Int. Ed.* **1997**, *36*, 840–842.
(24) Liu, D.; Lash, T. D. *J. Org. Chem.* **2003**, *68*, 1755–1761.
(25) Lash, T. D.; Muckey, M. A.; Hayes, M. J.; Liu, D.; Spence, J. D.; Ferrence, G. M. *J. Org. Chem.* **2003**, *68*, 8558–8570.
(26) Muckey, M. A.; Scczepura, L. F.; Ferrence, G. M.; Lash, T. D. *Inorg. Chem.* **2002**, *41*, 4840–4842.
(27) Lash, T. D.; Colby, D. A.; Szczepura, L. F. *Inorg. Chem.* **2004**, *43*, 5258–5267.
(28) Lash, T. D. *Org. Lett.* **2011**, *13*, 4632–4635.
(29) Szyszko, B.; Latos-Grazynski, L.; Szterenberg, L. *Angew. Chem., Int. Ed.* **2011**, *50*, 6587–6591.
(30) Furuta, H.; Maeda, H.; Osuka, A. *J. Org. Chem.* **2000**, *65*, 4222–4226.
(31) Furuta, H.; Maeda, H.; Osuka, A. *J. Org. Chem.* **2001**, *66*, 8563–8572.
(32) Toganoh, M.; Furuta, H. *J. Org. Chem.* **2013**, *78*, 9317–9327.
(33) Ghosh, A.; Wondimagegn, T.; Nilsen, H. J. *J. Phys. Chem. B* **1998**, *102*, 10459–10467.
(34) Ghosh, A. *Acc. Chem. Res.* **1998**, *31*, 189–198.
(35) Ghosh, A. In *The Porphyrin Handbook*; Kadish, K. M., Smith, K. M., Guilard, R., Eds.: Academic Press: San Diego, CA, 2000; Vol. *7*, pp 1–38.
(36) Liu, X.-J.; Feng, J.-K.; Ren, A.-M.; Zhou, X. *Chem. Phys. Lett.* **2003**, *373*, 197–206.
(37) Liu, X.-J.; Pan, Q.-J.; Meng, J.; Feng, J.-K. *J. Mol. Struct. (THEOCHEM)* **2006**, *765*, 61–69.
(38) Many of the structures shown in these two papers are incorrect, making it difficult to fully assess the results.
(39) Jelovica, I.; Moroni, L.; Gellini, C.; Salvi, P. R. *J. Phys. Chem. A* **2005**, *109*, 9935–9944.
(40) Loboda, O. *J. Chem. Inf. Model.* **2007**, *47*, 2266–2270.
(41) Schleyer, P. v. R.; Maerker, C.; Dransfeld, A.; Jiao, H.; Hommes, N. J. R. v. E. *J. Am. Chem. Soc.* **1996**, *118*, 6317–6318.
(42) (a) Poater, J.; Sola, M.; Viglione, R. G.; Zanasi, R. *J. Org. Chem.* **2004**, *69*, 7537–7542. (b) Lazzeretti, P. *Phys. Chem. Chem. Phys.* **2004**, *6*, 217–223. (c) Steiner, E.; Fowler, P. W. *Phys. Chem. Chem. Phys.* **2004**, *6*, 261–272. (d) Carion, R.; Champagne, B.; Monaco, G.; Zanasi, R.; Pelloni, S.; Lazzeretti, P. *J. Chem. Theory Comput.* **2010**, *6*, 2002–2018.
(43) Lash, T. D.; Lammer, A. D.; Ferrence, G. M. *Angew. Chem., Int. Ed.* **2012**, *51*, 10871–10875.
(44) Sprutta, N.; Mackowiak, S.; Kocik, M.; Szterenberg, L.; Lis, T.; Latos-Grazynski, L. *Angew. Chem., Int. Ed.* **2009**, *48*, 3337–3341.
(45) Frisch, M. J.; Trucks, G. W.; Schlegel, H. B.; Scuseria, G. E.; Robb, M. A.; Cheeseman, J. R.; Montgomery, J. A., Jr.; Vreven, T.; Kudin, K. N.; Burant, J. C.; Millam, J. M.; Iyengar, S. S.; Tomasi, J.; Barone, V.; Mennucci, B.; Cossi, M.; Scalmani, G.; Rega, N.; Petersson, G. A.; Nakatsuji, H.; Hada, M.; Ehara, M.; Toyota, K.; Fukuda, R.; Hasegawa, J.; Ishida, M.; Nakajima, T.; Honda, Y.; Kitao, O.; Nakai, H.; Klene, M.; Li, X.; Knox, J. E.; Hratchian, H. P.; Cross, J. B.; Bakken, V.; Adamo, C.; Jaramillo, J.; Gomperts, R.; Stratmann, R. E.; Yazyev, O.; Austin, A. J.; Cammi, R.; Pomelli, C.; Ochterski, J. W.; Ayala, P. Y.; Morokuma, K.; Voth, G. A.; Salvador, P.; Dannenberg, J. J.; Zakrzewski, V. G.; Dapprich, S.; Daniels, A. D.; Strain, M. C.; Farkas, O.; Malick, D. K.; Rabuck, A. D.; Raghavachari, K.; Foresman, J. B.; Ortiz, J. V.; Cui, Q.; Baboul, A. G.; Clifford, S.; Cioslowski, J.; Stefanov, B. B.; Liu, G.; Liashenko, A.; Piskorz, P.; Komaromi, I.; Martin, R. L.; Fox, D. J.; Keith, T.; Al-Laham, M. A.; Peng, C. Y.; Nanayakkara, A.; Challacombe, M.; Gill, P. M. W.; Johnson, B.; Chen,

W.; Wong, M. W.; Gonzalez, C.; Pople, J. A. *Gaussian 03, Revision C.02*; Gaussian, Inc., Wallingford, CT, 2004.
(46) Wolinski, K.; Hinton, J. F.; Pulay, P. *J. Am. Chem. Soc.* **1990**, *112*, 8251−8260.